JOURNAL OF RESEARCH of the National Bureau of Standards—A. Physics and Chemistry
Vol. 73A, No. 4, July-August 1969

The System SrO—"Chromium Oxide" in Air and Oxygen

Taki Negas and Robert S. Roth

Institute for Materials Research, National Bureau of Standards, Washington, D.C. 20234

(April 25, 1969)

Phase relations in the system SrO-"chromium oxide" were determined in air and 1 atm O_2 (1 atm = 1.013×10^5 N/m²) and are shown as isobaric projections on the SrO—Cr_2O_3 pseudobinary. At both oxygen pressures, the system consists of three joins in the SrO—Cr_2O_3-oxygen ternary, (1) SrO—$Sr_3Cr_2O_8$, (2) $Sr_3Cr_2O_8$—$SrCrO_4$, and (3) $SrCrO_4$—Cr_2O_3. The former is binary from 1065 °C to liquidus temperatures in air and includes a eutectic near 79 mol percent SrO (in terms of SrO—Cr_2O_3 starting materials). $Sr_3Cr_2O_8$ melts congruently at 1453 °C. Below 1065 °C in air, phase relations are complicated by reactions with atmospheric water vapor resulting in the formation of $Sr_{10}Cr_6O_{24}(OH)_2$ which decomposes to SrO and $Sr_3Cr_2O_8$ above 1065 °C. In air, below 775 °C, $Sr_3Cr_2O_8$ reacts with water vapor and oxygen to form $Sr_{10}Cr_6O_{24}(OH)_2$ and $SrCrO_4$. Water vapor reactions are restricted in 1 atm O_2. The $Sr_3Cr_2O_8$—$SrCrO_4$ join contains a binary eutectic between 69–70 mol percent SrO but liquidus relations are ternary below 69 (air) and 68 (oxygen) mol percent SrO, as reduction of Cr^{6+} occurs. Likewise, the $SrCrO_4$—Cr_2O_3 join is not binary at solidus and liquidus temperatures. In air, $SrCrO_4$ melts at 1251 °C to Cr_2O_3 plus liquid with release of oxygen. In oxygen, the compound melts at 1283 °C with evolution of oxygen.

Key words: Chromium oxide; phase equilibria; strontium chromates; strontium-"chromium oxide" system, $SrCrO_4$, $Sr_3Cr_2O_8$.

1. Introduction

Investigation of phase relations in the system SrO-"chromium oxide" was initiated as part of a program of phase equilibrium studies involving the high temperature oxidation-reduction behavior of the first-row transition series metals. Although a number of mixed oxide compounds of strontium and chromium are reported in the literature [1–6],[1] systematic attempts to deduce phase relations as a function of temperature and controlled oxygen pressure were not made. This paper presents two oxygen isobaric sections, air (0.21 atm O_2) and 1 atm O_2 (1 atm = 1.013×10^5 N/m²), through the SrO—Cr_2O_3-oxygen ternary which is a subsystem of the Sr—Cr-oxygen ternary. X-ray diffraction and gravimetric data together with determinations of the melting points of compounds and of solidus and liquidus temperatures for various compositions in the system were used to construct the two isobaric sections. For convenience, phase relations in the ternary are depicted as projections on the SrO—Cr_2O_3 preudobinary but do not necessarily reflect equilibria for compositions confined to the pseudobinary. Although ternary in nature, the SrO—Cr_2O_3 pseudobinary may be interpreted in the normal binary manner because of the assignment of a fixed P_{O_2}.

[1] Figures in brackets indicate the literature references at the end of this paper.

2. Sample Preparation and Experimental Procedure

Strontium carbonate was used as the source for the alkaline earth metal and highly reactive Cr_2O_3, prepared from $Cr(NO_3)_3 \cdot 9H_2O$ by gentle ignition, for chromium. Compositions were calculated to ±0.01 percent and included a weight loss factor for $SrCO_3$. Starting materials in sufficient quantities to yield 3.0 g batches were weighed to the nearest 0.1 mg. Each batch was mixed in a mechanical shaker, dry mixed by hand, and pressed into a disk in a $\frac{5}{8}$-in diam mold at 10,000 lb/in². The disks were fired, with periodic remixing and pressing, at 850 °C in air in a horizontal muffle furnace for 100 hr.

Melting point and subsolidus data were obtained by the quenching method from calcined samples equilibrated at constant temperature and pressure in open platinum tubes. In some cases, open gold envelopes or Vycor tubes were used. A vertical tube resistance-type furnace wound with 80 percent Pt–20 percent Rh wire was used for equilibrations in air. Specimens were equilibrated at 1 atm O_2 in a similar furnace modified for vacuum and gas flow capability with end-closures and "O"-ring seals. High purity oxygen was passed at a flow rate of 60 cm³/min through a kerosene-solid CO_2 cold trap into the furnace and out to the atmosphere through a second cold trap followed by a glass "bubbler" containing a 1-in water column.

The furnace was twice evacuated to 3×10^{-4} atm and flushed with oxygen before each experiment.

Temperatures were measured with Pt-Pt 10 percent Rh thermocouples calibrated against the melting points of NaCl (801 °C), Au (1063 °C), and Pd (1552 °C) [7]. The furnaces were controlled by an a–c Wheatstone bridge controller capable of maintaining temperature to at least ± 2 °C.

Air-heated specimens were quenched onto a cold metal tray while those equilibrated in oxygen were quenched into a "dry ice" cooled brass cold-finger that constitutes the lower portion of the furnace. After quenching, specimens were examined under a binocular microscope for physical appearances of melting and x-ray powder patterns were made. Glazing accompanied by direct, but limited, specimen to Pt-container-surface contact was interpreted as the first experimental evidence for solidus temperatures. High chromium content specimens (> 33 mol percent Cr_2O_3) also displayed small cavities indicative of gas release at solidus temperatures as well as minor changes in x-ray powder patterns. Liquidus temperatures were more difficult to deduce but were generally characterized by the development of a deeply concave meniscus indicative of a highly mobile material. Chromium-rich specimens were particularly difficult to retain in their containers as high fluidity was enhanced by gas release. The overall reproducibility of the temperature measurements for the experimental data points is within ±2 °C and the overall accuracy of the reported temperatures is within ±5 °C.

Equilibrium was considered to have been attained when the x-ray diffraction patterns of specimens heated successively for longer times and/or at higher temperature did not change. X-ray powder patterns were made using a high-angle Geiger counter-diffractometer at 1/4° 2θ/min scanning rate and nickel-filtered Cu radiation. Reported unit cell data are considered accurate to about ± 2 in the last decimal place given.

The air and 1 atm O_2 liquidus isobars were determined by weight regain measurements. One-half to 1-½ g specimens were equilibrated within 5 °C above their liquidus temperature and quenched. After weighing at room temperature they were reoxidized by heating at a subsolidus temperature in air where phase assemblage and bulk composition were known from previous experiments. These were reweighed at room temperature after sufficient heating to permit complete reversal. Weight gain at the subsolidus temperature, therefore, represented weight loss for an equivalent amount of specimen at the liquidus temperature.

3. Compounds

The system SrO-"chromium oxide" contains few compounds in air or 1 atm O_2. The phase $Sr_3Cr_2O_8$ has been reported [2,3,8,9,10,11] and is trigonal with s.g. (space group) $R\bar{3}m$. It is isostructural with $Ba_3P_2O_8$ [12] and contains the unusual Cr^{5+} state. The hexagonal cell dimensions for the compound in this study, $a = 5.569$ Å and $c = 20.17$ Å, are in accord with those of Scholder and Schwarz [2] and Wilhelmi and Jonsson [3].

Pistorius and Pistorius [1] reported $SrCrO_4$ (monoclinic, s.g. $P2_1/n$, $a = 7.083$ Å, $b = 7.388$ Å, $c = 6.771$ Å, $\beta = 103.43°$) which is isostructural with $PbCrO_4$. Cell parameters for the $SrCrO_4$ in this study, $a = 7.09$ Å, $b = 7.40$ Å, $c = 6.74$ Å, $\beta = 103.3°$, are in good agreement with the above.

The compounds $SrCr_2O_7$ [4], $Sr_2Cr^{4+}O_4$ [5], and $SrCr^{4+}O_3$ [6] do not appear in the system at 0.21 and 1 atm O_2. The former is probably a higher P_{O_2}-low temperature phase. Sr_2CrO_4 was prepared in this laboratory at 1215 °C (44 hr) and 2×10^{-5} atm and is, therefore, a low P_{O_2} phase with Cr^{4+} in tetrahedral coordination while $SrCrO_3$ is a high pressure cubic perovskite with Cr^{4+} in octahedral coordination.

Phase relations at low temperatures in air of compositions within the SrO-rich portion of the system are severely influenced by atmospheric water vapor. The compound $Sr_{10}Cr_6O_{24}(OH)_2$, a hydroxyapatite, readily develops and persists to elevated temperatures before decomposing with H_2O evolution at about 1065 °C to SrO and $Sr_3Cr_2O_8$. Scholder and Schwarz [2] and Banks and Jaunarajs [13] prepared a Sr—Cr hydroxyapatite (*hex*, s.g. $P6_3/m$, $a = 10.009$ Å, $c = 7.435$ Å and $a = 9.98$ Å, $c = 7.40$ Å, respectively). According to Scholder and Suchy [14] magnetochemical analysis yielded data indicating that pentavalent Cr exists in the compound, as well as in Ba and Ca analogs, instead of a 2:4 disproportionation of Cr^{3+} and Cr^{6+}. The apatite phase found in this study is hexagonal with $a = 10.009$ Å and $c = 7.427$ A. To investigate the possibility that this compound might be of the oxyapatite-type, $Sr_{10}Cr_6^{5+}O_{24}O$, rather than a hydroxyl phase which, more appropriately, belongs to the SrO—Cr_2O_3—O_2—H_2O quaternary, a qualitative analysis

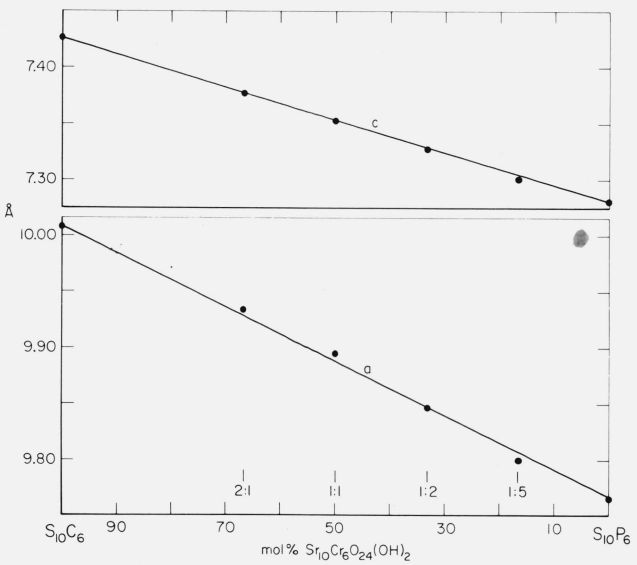

FIGURE 1. *Unit cell parameters of* $Sr_{10}(CrO_4)_{2\times}(PO_4)_{6-2\times}(OH)_2$ *solid solutions prepared at 900 °C in air.*
($S_{10}C_6$=$Sr_{10}Cr_6O_{24}(OH)_2$, $S_{10}P_6$ = $Sr_{10}P_6O_{24}(OH)_2$)

was made for protons on material made at 1000 °C on gold using broadline nuclear magnetic resonance. The analysis suggested a large concentration of protons. Furthermore, the possible reactions

(a) $3Sr_3Cr_2O_8 + SrO + H_2O \rightarrow Sr_{10}Cr_6O_{24}(OH)_2$
(b) $3Sr_3Cr_2O_8 + SrO \rightarrow Sr_{10}Cr_6O_{24}O$

were tested gravimetrically by heating $Sr_3Cr_2O_8 + SrO$ at 850 °C in air. Equation (a) suggests a theoretical weight gain of 1.13 percent while (b) involves no weight change. A measured value of 1.08 percent suggested reaction (a). A specimen decomposed to $SrO + Sr_3Cr_2O_8$ at 1225 °C, sealed in a Pt tube, and reheated at 825 °C, did not reverse, also suggesting reaction (a). Additional evidence for the existence of a Cr^{5+} hydroxyapatite is the isotypism with $Sr_{10}P_6O_{24}(OH)_2$ as demonstrated by the formation of ideal solid solutions, $Sr_{10}(CrO_4)_{2x}(PO_4)_{6-2x}(OH)_2$, at 900 °C in air (fig. 1).

4. Discussion of Phase Equilibria

Phase relations in air (0.21 atm O_2) and 1 atm O_2 are shown in figures 2, 3, 4, and 5. The data from which these diagrams were constructed are given in tables 1 and 2. The system is not truly binary in its entirety because of reactions with oxygen but consists of a number of ternary elements (figs. 2 and 4) which may be projected onto the $SrO—Cr_2O_3$ pseudobinary (figs. 3 and 5), or any other convenient compositional reference join, through lines of constant cation-cation ratio but variable oxygen content (oxygen reaction lines).

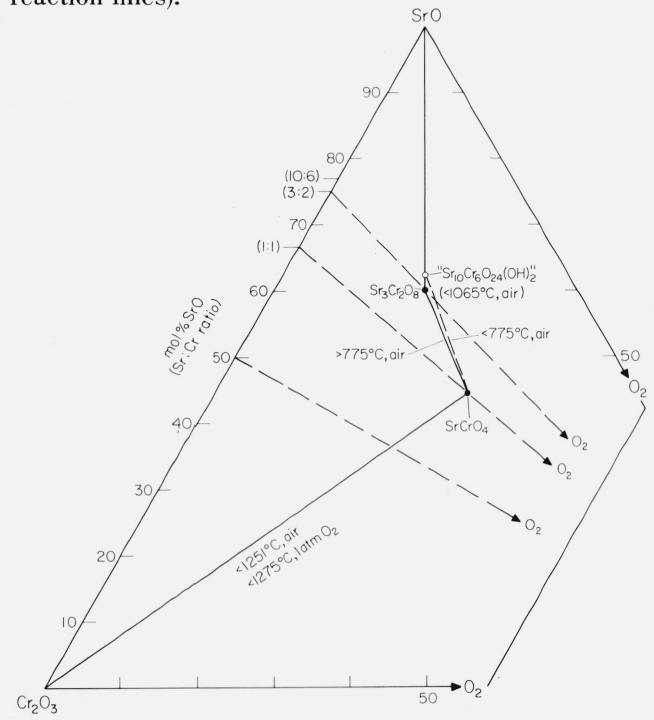

FIGURE 2. *Air and 1 atm O_2 subsolidus relations in the system $SrO—Cr_2O_3—O_2$.*

4.1. Air Equilibria

a. The $SrO—Sr_3Cr_2O_8$ Join and Related Equilibria

The 0.21 atm isobar coincides at subsolidus temperatures (> 1065 °C) and liquidus temperatures with the $SrO—Sr_3Cr_2O_8$ join; the join is a true binary in air at all temperatures above 1065 °C to at least the liquidus. Apatite, $Sr_{10}Cr_6O_{24}(OH)_2$, does not belong to this join but lies in the $SrO—Sr_3Cr_2O_8—H_2O$ subternary of the $SrO—Cr_2O_3—O_2—H_2O$ quanternary but is nevertheless indicated, because of its influence on phase relations, as a projection onto the $SrO—Sr_3Cr_2O_8$ join in figure 2 and with dashed lines at the 10:3 $SrO:Cr_2O_3$ ratio in figure 3. Between 1065 and 775 °C phase relations for compositions between SrO and the 3:2 cation-cation ratio actually consist of:

(a) $SrO—Sr_{10}Cr_6O_{24}(OH)_2$: a tie line extending above the plane of the ternary toward a hypothetical H_2O apex and connecting SrO and the composition of apatite.
(b) $Sr_{10}Cr_6O_{24}(OH)_2—Sr_3Cr_2O_8$; a tie line extending from the composition of apatite to that of $Sr_3Cr_2O_8$.

Above 1065 °C, the apatite phase decomposes to $Sr_3Cr_2O_8$ plus SrO with H_2O evolution thereby establishing the $SrO—Sr_3Cr_2O_8$ tie line. An unusual reaction not indicated in figures 2 and 3 but involving the apatite, occurs below approximately 635 °C. The reaction is very sluggish because of the low temperature. Dehydroxylation of apatite proceeds not because of instability due to high temperature but as a result of low temperature oxidation of Cr^{5+} to Cr^{6+} according to

$$Sr_{10}Cr^{5+}_6O_{24}(OH)_2 + 1\tfrac{1}{2}O_2 \rightarrow 6SrCr^{6+}O_4 + 4SrO + H_2O.$$

The available SrO reacts with CO_2 at low temperatures and is readily identified in x-ray powder patterns as $SrCO_3$.

$Sr_3Cr_2O_8$ melts congruently at 1453 °C and a binary eutectic occurs between 79–80 mol percent SrO and 1365 °C. The liquidus curve delimiting the primary field of SrO shows a pronounced "flattening" which could not be followed using compositions more SrO-rich than 85 mol percent. These tend to react with the platinum container to form Sr_4PtO_6 [15]. In fact, the "flattening" tendency and the magnitude of the solidus temperature are probably the result of traces of Sr_4PtO_6. Materials more SrO-rich than $Sr_3Cr_2O_8$ could be prepared free of Sr_4PtO_6 only by heating multiple disks of specimens resting on two strands of fine Pt wire wrapped about an alumina dish. The disks were located at the open end of the dish to prevent contact with the alumina.

$Sr_3Cr_2O_8$ has a "minimum" at approximately 775 °C below which it reacts with atmospheric oxygen and water vapor according to:

$$4Sr_3Cr_2O_8 + \tfrac{1}{2}O_2 + H_2O \rightarrow Sr_{10}Cr_6O_{24}(OH)_2 + 2SrCrO_4$$

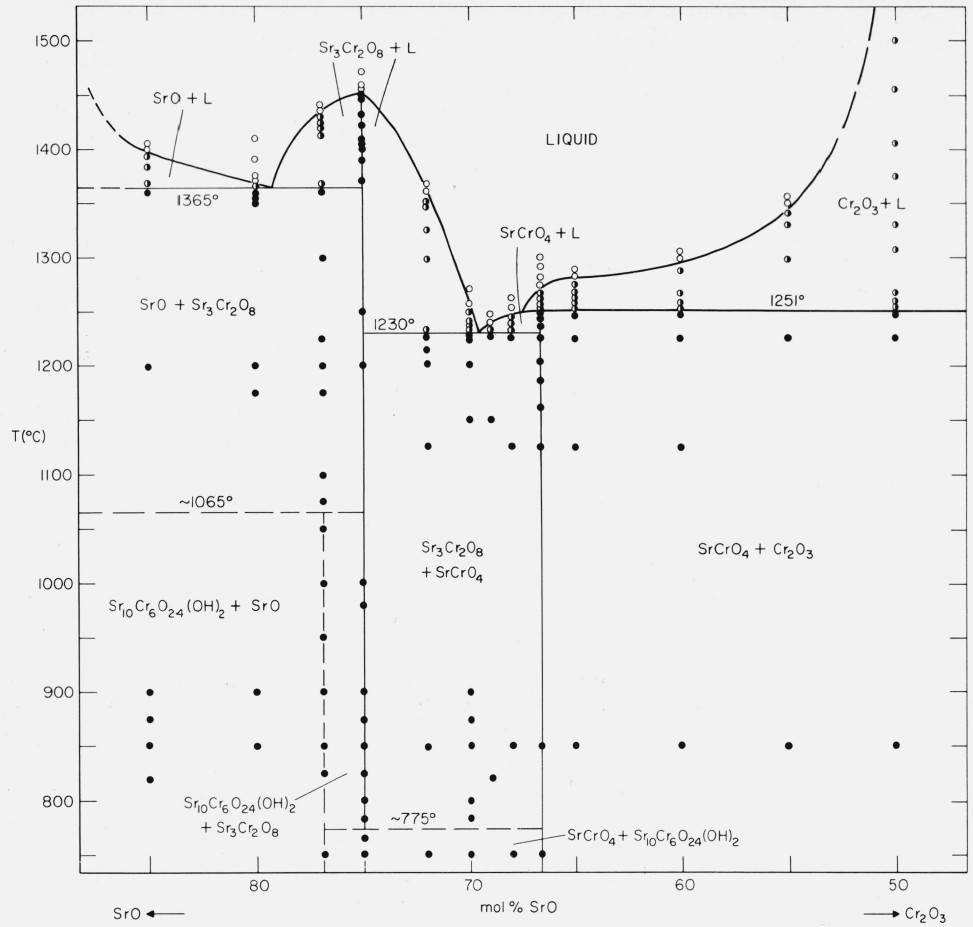

FIGURE 3. *Phase relations in the system* SrO-"*chromium oxide*," *in air, projected on the* SrO—Cr_2O_3 *pseudobinary.*
(●—solid; ◑—partly melted; ○—liquid.)

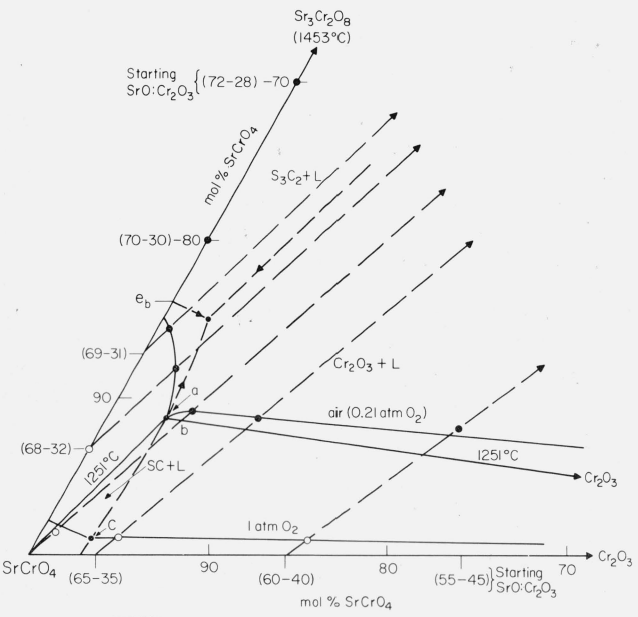

FIGURE 4. *The air and 1 atm* O_2 *liquidus isobars in the* $Sr_3Cr_2O_8$—$SrCrO_4$—Cr_2O_3 *subternary of the system* SrO-"*chromium oxide.*"
(●—air; ○—1 atm O_2; dashed straight lines with arrows are lines of constant Sr—Cr ratio; e_b is a binary eutectic; dashed curved lines with arrows are boundary curves; S_3C_2=$Sr_3Cr_2O_8$; SC=$SrCrO_4$.)

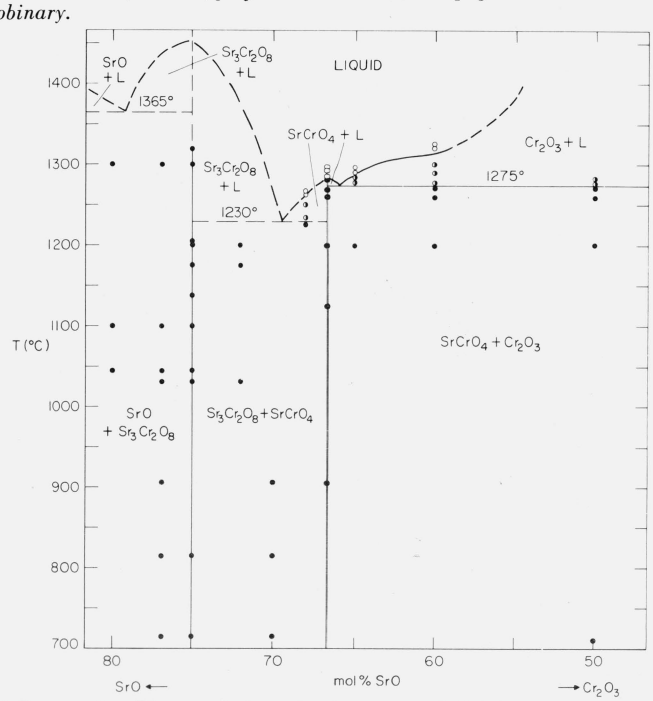

FIGURE 5. *Phase relations in the system* SrO-"*chromium oxide*" *at 1 atm* O_2, *projected on the* SrO—Cr_2O_3 *pseudobinary.*
(●—solid; ◑—partly melted; ○—liquid.)

TABLE 1. *Experimental data for the system* SrO-"*chromium oxide*"

Heat treatments [a]								Results	
Composition		Initial		Final (air)		Final (O_2) [b]		Physical State	X-ray analysis [c]
SrO	Cr_2O_3	Temp.	Time	Temp.	Time	Temp.	Time		
mol %	*mol %*	*°C*	*hr*	*°C*	*hr*	*°C*	*hr*		
85	15	850	100						$S_{10}C_6 + SrCO_3$
				820	22				$S_{10}C_6 + SrCO_3$
				875	60				$S_{10}C_6 + SrCO_3$
		1200	60						$S_3C_2 + S$
				900	60				$S_{10}C_6 + S$
				1363	1			No melting	$S_3C_2 + S$
				1367	1			Partial melting	$S_3C_2 + S$
				1384	1			Partial melting	$S_3C_2 + S$
				1394	1			Partial melting	$S_3C_2 + S$
				1399	0.75			Completely melted (?)	$S_3C_2 + S$
				1404	1			Completely melted	$S_3C_2 + S$
80	20	850	100						
				900	60				$S_{10}C_6 + SrCO_3$
						1045	20		$S_3C_2 + S + tr \cdot S_4P$
						1100	20		$S_3C_2 + S + tr \cdot S_4P$
						1300	5		$S_3C_2 + S + tr \cdot S_4P$
		1200	60						$S_3C_2 + S$
				1175	4				$S_3C_2 + S$
				1351	1			No melting	$S_3C_2 + S$
				1357	1			No melting	$S_3C_2 + S$
				1361	1			No melting	$S_3C_2 + S$
				1364	1			No melting	$S_3C_2 + S$
				1366	1			Partial melting	$S_3C_2 + S$
				1367	1			Partial melting	$S_3C_2 + S$
				1371	1			Completely melted	$S_3C_2 + S$
				1375	1			Completely melted	$S_3C_2 + S$
				1391	1			Completely melted	$S_3C_2 + S$
				1410	1			Completely melted	$S_3C_2 + S$
76.92	13.08	850	100						$S_{10}C_6$
				[d]500	48				$S_{10}C_6 + SC + SrCO_3$
				[d]600	120				$S_{10}C_6 + SC + SrCO_3$
				[d]625	96				$S_{10}C_6 + SC + SrCO_3$
				[d]650	122				$S_{10}C_6$
				[d]700	100				$S_{10}C_6$
				[d]750	100				$S_{10}C_6$
				[d]900	60				$S_{10}C_6$
				[d]950	70				$S_{10}C_6$
				[d]1000	70				$S_{10}C_6$
				[d]1050	70				$S_{10}C_6$
				[e]1075	4				$S_{10}C_6 + S_3C_2 + S$
				[e]1100	25				$S_3C_2 + S$
				1175	4				$S_3C_2 + S$
				1225	19				$S_3C_2 + S$
						[d]714	120		$S_3C_2 + S$
						[d]1032	120		$S_3C_2 + S$
		1200	60						$S_3C_2 + S$
				[f]825	65				$S_3C_2 + S$
				[d]900	60				$S_{10}C_6$
				[d]950	70				$S_{10}C_6 + tr \cdot S_3C_2$
				[d]1000	70				$S_{10}C_6 + tr \cdot S_3C_2$
				[d]1050	70				$S_{10}C_6 + tr \cdot S_3C_2$
				[e]1075	4				$S_3C_2 + S$

TABLE 1. *Experimental data for the system* SrO-"*chromium oxide*" —Continued

Heat treatments [a]								Results	
Composition		Initial		Final (air)		Final (O_2) [b]		Physical State	X-ray analysis [c]
SrO	Cr_2O_3	Temp.	Time	Temp.	Time	Temp.	Time		
mol %	*mol %*	*°C*	*hr*	*°C*	*hr*	*°C*	*hr*		
				[e] 1100	25				$S_3C_2 + S$
				1300	50			No melting	$S_3C_2 + S$
				1363	1			No melting	$S_3C_2 + S$
				1367	1			Partial melting	$S_3C_2 + S$
				1413	1			Partial melting	$S_3C_2 + S$
				1419	1			Partial melting	$S_3C_2 + S$
				1425	1			Partial melting	$S_3C_2 + S$
				1430	1			Partial melting	$S_3C_2 + S$
				1435	1			Completely melted	$S_3C_2 + S$
				1442	1			Completely melted	$S_3C_2 + S$
						[d] 714	120		$S_3C_2 + S$
						[d] 815	70		$S_3C_2 + S$
						[d] 906	120		$S_3C_2 + S$
						[d] 1032	120		$S_3C_2 + S$
						1045	20		$S_3C_2 + S + tr \cdot S_4P$
						1100	20		$S_3C_2 + S + tr \cdot S_4P$
						1300	5		$S_3C_2 + S + tr \cdot S_4P$
75	25	850	100						
		750	100						
				750	24				$S_{10}C_6 + SC$
				765	65				$S_{10}C_6 + SC$
				785	40				$S_{10}C_6 + S_3C_2 + SC$
				800	90				$S_3C_2 + tr \cdot S_{10}C_6 + tr \cdot SC$
				825	25				$S_3C_2 + tr \cdot S_{10}C_6 + tr \cdot SC$
				850	18				$S_3C_2 + tr \cdot S_{10}C_6 + tr \cdot SC$
				875	18				$S_3C_2 + tr \cdot S_{10}C_6 + tr \cdot SC$
				900	16				S_3C_2
				980	18				S_3C_2
				1000	18				S_3C_2
						[d] 714	120		S_3C_2
						[d] 815	70		S_3C_2
						1045	20		$S_3C_2 + tr \cdot S_4P$
						1100	20		$S_3C_2 + tr \cdot S_4P$
						1138	70		$S_3C_2 + tr \cdot S_4P$
						1200	4		S_3C_2
						1205	49		S_3C_2
						1300	5		S_3C_2
						1320	72		S_3C_2
		1200	60						S_3C_2
				750	24				$S_{10}C_6 + S_3C_2 + SC$
				765	65				$S_{10}C_6 + S_3C_2 + SC$
				785	40				S_3C_2
				800	90				S_3C_2
				900	16				S_3C_2
				1250	15			No melting	S_3C_2
				1370	1			No melting	S_3C_2
				1390	1			No melting	S_3C_2
				1400	2			No melting	S_3C_2
				1404	1			No melting	S_3C_2
				1409	1			No melting	S_3C_2
				1425	1			No melting	S_3C_2
				1432	1			No melting	S_3C_2
				1449	1			No melting	S_3C_2
				1452	1			Partial melting (?)	S_3C_2
				1455	1			Completely melted	S_3C_2
				1459	1			Completely melted	S_3C_2
				1471	1			Completely melted	S_3C_2
						1032	120		S_3C_2
						1175	120		S_3C_2

TABLE 1. *Experimental data for the system* SrO-"*chromium oxide*" —Continued

Heat treatments [a]								Results	
Composition		Initial		Final (air)		Final (O_2) [b]		Physical State	X-ray analysis [c]
SrO	Cr_2O_3	Temp.	Time	Temp.	Time	Temp.	Time		
mol %	*mol %*	*°C*	*hr*	*°C*	*hr*	*°C*	*hr*		
72	28	850	100						
				750	100				$S_{10}C_6 + SC$
						1032	120		$S_3C_2 + SC$
						1175	3		$S_3C_2 + SC$
						1200	4		$S_3C_2 + SC$
		1125	60						$S_3C_2 + SC$
				1202	2			No melting	$S_3C_2 + SC$
				1215	2			No melting	$S_3C_2 + SC$
				1227	1			No melting	$S_3C_2 + SC$
				1232	1			Partial melting	$S_3C_2 + SC$
				1299	1			Partial melting	$S_3C_2 + SC$
				1326	1			Partial melting	$S_3C_2 + SC$
				1349	1			Partial melting	$S_3C_2 + SC$
				1351	1			Partial melting	$S_3C_2 + SC$
				1362	1			Completely melted	$S_3C_2 + SC$
				1369	1			Completely melted	$S_3C_2 + SC$
70	30	850	100						
				750	100				$SC + S_{10}C_6$
				785	40				$SC + S_3C_2 + tr \cdot S_{10}C_6$
				800	90				$SC + S_3C_2 + tr \cdot S_{10}C_6$
				850	18				$SC + S_3C_2 + tr \cdot S_{10}C_6$
						714	120		$SC + S_3C_2$
						815	70		$SC + S_3C_2$
						906	120		$SC + S_3C_2$
		1150	48						$SC + S_3C_2$
				750	24				$SC + S_{10}C_6 + tr \cdot S_3C_2$
				785	40				$SC + S_3C_2$
				800	90				$SC + S_3C_2$
				900	16				$SC + S_3C_2$
				1202	2			No melting	$SC + S_3C_2$
				1225	1			No melting	$SC + S_3C_2$
				1228	1			No melting	$SC + S_3C_2$
				1232	1			Partial melting	$SC + S_3C_2$
				1236	1			Partial melting	$SC + S_3C_2$
				1240	1			Partial melting	$SC + S_3C_2$
				1249	1			Partial melting (?)	$SC + S_3C_2$
				1257	1			Completely melted	$SC + S_3C_2$
				1273	1			Completely melted	$SC + S_3C_2$
69	31	820	20						
		1150	50						$SC + S_3C_2$
				1228	1			No melting	$SC + S_3C_2$
				1233	1			Partial melting	$SC + S_3C_2$
				1240	1			Completely melted (?)	$SC + S_3C_2$
				1247	1			Completely melted	$SC + S_3C_2$
68	32	850	100						
				750	24				$SC + S_{10}C_6 + tr \cdot S_3C_2$
		1125	60						$SC + S_3C_2$
				1227	1			No melting	$SC + S_3C_2$
				1232	1			Partial melting	$SC + S_3C_2$
				1239	1			Partial melting	$SC + S_3C_2$

349-367 O-69—4

TABLE 1. *Experimental data for the system* SrO-"*chromium oxide*" —Continued

Heat treatments [a]								Results	
Composition		Initial		Final (air)		Final (O_2) [b]		Physical State	X-ray analysis [c]
SrO	Cr_2O_3	Temp.	Time	Temp.	Time	Temp.	Time		
mol %	*mol %*	*°C*	*hr*	*°C*	*hr*	*°C*	*hr*		
				1246	1			Partial melting	SC + S_3C_2
				1256	1			Completely melted	SC + S_3C_2
				1263	1			Completely melted	SC + S_3C_2
						1228	5	No melting	SC + S_3C_2
						1234	5	Partial melting	SC + S_3C_2
						1252	5	Partial melting	SC + S_3C_2
						1262	16	Completely melted	SC + S_3C_2
						1266	5	Completely melted	SC + S_3C_2
66.67	33.33	850	100						
				750	100				SC
				1125	60			No melting	SC
				1162	16			No melting	SC
				1186	15			No melting	SC
				1204	1			No melting	SC
				1227	1			No melting	SC
				1238	16			No melting	SC
				1243	5			No melting	SC
				1245	1			No melting	SC
				1249	1			No melting	SC
				1252	1			Partial melting	SC + tr · S_3C_2
				1255	1			Partial melting	SC + tr · S_3C_2
				1263	1			Partial melting	SC + tr · S_3C_2
				1269	1			Partial melting	SC + tr · S_3C_2 + tr · C
				1274	1			Completely melted	SC + tr · S_3C_2 + tr · C
				1282	1			Completely melted	SC + tr · S_3C_2 + tr · C
				1292	1			Completely melted	SC + tr · S_3C_2 + tr · C
				1301	1			Completely melted	SC + tr · S_3C_2 + tr · C
						906	120	No melting	SC
						1125	70	No melting	SC
						1200	4	No melting	SC
						1260	2	No melting	SC
						1270	2	No melting	SC
						1281	2	No melting	SC
						1285	1	Completely melted	SC + tr · S_3C_2
						1294	1.25	Completely melted	SC + tr · S_3C_2
						1296	1	Completely melted	SC + tr · S_3C_2
65	35	850	100						
				1125	60				SC + C
				1225	15			No melting	SC + C
				1247	1			No melting	SC + C
				1253	1			Partial melting	SC + C + tr · S_3C_2
				1257	1			Partial melting	SC + C + tr · S_3C_2
				1261	1			Partial melting	SC + C + tr · S_3C_2
				1266	1			Partial melting	SC + C + tr · S_3C_2
				1274	1			Partial melting	SC + C + tr · S_3C_2
				1284	1			Completely melted	SC + C + tr · S_3C_2
				1288	1			Completely melted	SC + C + tr · S_3C_2
						1200	3	No melting	SC + C
						1278	1.25	Partial melting	SC + C
						1285	1.25	Partial melting	SC + C + tr · S_3C_2
						1290	1.25	Completely melted	SC + C + tr · S_3C_2
						1297	1.25	Completely melted	SC + C + tr · S_3C_2
60	40	850	100						
				1125	60				SC + C
				1225	15			No melting	SC + C
				1248	1			No melting	SC + C
				1253	1			Partial melting	SC + C + tr · S_3C_2
				1257	1			Partial melting	SC + C + tr · S_3C_2

TABLE 1. *Experimental data for the system* SrO-"*chromium oxide*" — Continued

Heat treatments [a]								Results	
Composition		Initial		Final (air)		Final (O_2) [b]		Physical State	X-ray analysis [c]
SrO	Cr_2O_3	Temp.	Time	Temp.	Time	Temp.	Time		
mol %	*mol %*	*°C*	*hr*	*°C*	*hr*	*°C*	*hr*		
				1268	1			Partial melting	SC + C + tr · S_3C_2
				1287	1			Partial melting	SC + C + tr · S_3C_2
				1298	1			Completely melted	SC + C + tr · S_3C_2
				1306	1			Completely melted	SC + C + tr · S_3C_2
						1200	3	No melting	SC + C
						1259	1.25	No melting	SC + C
						1273	1.25	No melting	SC + C
						1277	1.25	Partial melting	SC + C
						1290	1.25	Partial melting	SC + C + tr · S_3C_2
						1300	1.25	Partial melting	SC + C + tr · S_3C_2
						1321	1.25	Completely melted	SC + C + tr · S_3C_2
						1325	1.25	Completely melted	SC + C + tr · S_3C_2
55	45	850	100						
				1225	15			No melting	SC + C
				1298	1			Partial melting	SC + C + tr · S_3C_2
				1328	1			Partial melting	SC + C + tr · S_3C_2
				1341	1			Partial melting (?)	SC + C + tr · S_3C_2
				1351	1			Completely melted	SC + C + tr · S_3C_2
				1355	1			Completely melted	SC + C + tr · S_3C_2
50	50	850	100						
				1225	15			No melting	SC + C
				1247	1			No melting	SC + C
				1254	1			Partial melting	SC + C + tr · S_3C_2
				1258	1			Partial melting	SC + C + tr · S_3C_2
				1267	1			Partial melting	SC + C + tr · S_3C_2
				1307	1			Partial melting	SC + C + tr · S_3C_2
				1330	1			Partial melting	SC + C + tr · S_3C_2
				1374	1			Partial melting	SC + C + tr · S_3C_2
				1405	1			Partial melting	SC + C + tr · S_3C_2
				1455	1			Partial melting	SC + C + tr · S_3C_2
				1500	1			Partial melting	SC + C + tr · S_3C_2
						710	46		SC + C
						1200	3	No melting	SC + C
						1259	1.25	No melting	SC + C
						1273	1.25	No melting	SC + C
						1277	1.25	Partial melting	SC + C
						1281	1	Partial melting	SC + C + tr · S_3C_2

[a] After the initial heat treatment(s) all specimens were reheated in open Pt tubes, unless otherwise indicated.
[b] 1 atmosphere.
[c] Phases identified are given in the order of amount present at room temperature. They are not necessarily those present at the temperature at which the specimen was heated.
[d] Open gold envelope.
[e] Open Vycor tube.
[f] Sealed Pt tube.
(?) — interpretation uncertain. S = SrO $S_3C_2 = Sr_3Cr_2O_8$ $S_{10}C_6 = Sr_{10}Cr_6O_{24}(OH)_2$ SC = $SrCrO_4$ C = Cr_2O_3 $S_4P = Sr_4PtO_6$, formed by reaction with Pt tube

This reaction is represented in figure 3 by the 775 °C horizontal. For compositions between apatite and $SrCrO_4$ the apatite-$SrCrO_4$ tie line, therefore, exists below 775 °C.

b. $Sr_3Cr_2O_8$—$SrCrO_4$—Cr_2O_3 Equilibria

Above 775 °C, to liquidus temperatures, compositions between $Sr_3Cr_2O_8$ and $SrCrO_4$ behave in a binary fashion at least to about 70 mol percent SrO. The $Sr_3Cr_2O_8$—$SrCrO_4$ tie line in figure 2 suggests binary behavior in the subsolidus. The invariant point between 70–69 mol percent SrO at 1230 °C is a true binary eutectic. Compositions more Cr-rich than $SrCrO_4$ behave in a binary manner only below the 1251 °C solidus as suggested by the $SrCrO_4$—Cr_2O_3 tie line in figure 2. The 0.21 atm O_2 liquidus isobar coincides only with a portion of the $Sr_3Cr_2O_8$—$SrCrO_4$ join and lies entirely off the $SrCrO_4$—Cr_2O_3 tie line within the $Sr_3Cr_2O_8$—$SrCrO_4$—Cr_2O_3 subternary (fig. 4.). This situation is created by the "incongruent" melting behavior of $SrCrO_4$ at 1251 °C. The compound melts to Cr_2O_3 plus liquid with evolution of oxygen as the result of reduction of Cr^{6+} to Cr^{3+} and Cr^{5+}. The

TABLE 2. *Summary of gravimetric experiments for the location of the air and 1 atm O_2 liquidus isobars in the $Sr_3Cr_2O_8$—$SrCrO_4$—Cr_2O_3 subternary*

Initial composition					Heat treatments [a]						
					Air		Oxygen				
SrO	Cr_2O_3	Subsolidus phases			Temp.	Time	Temp.	Time	Liquidus composition [b]		
mol %	*mol %*	*Bulk*		*mol %*	*°C*	*hr*	*°C*	*hr*	*Bulk* [c]	*Ternary phases* [d]	*mol %*
72	28	$Sr_{16}Cr_{13}O_{52}$	S_3C_2	30	1360	5			no change		
			SC	70							
70	30	$Sr_{14}Cr_{12}O_{48}$	S_3C_2	20	1256	5			no change		
			SC	80							
69	31	$Sr_{69}Cr_{62}O_{248}$	S_3C_2	12.73	1242	5			$Sr_{69}Cr_{62}O_{246.25}$	S_3C_2	14.27
			SC	87.27						SC	85.08
										C	0.65
68	32	$Sr_{85}Cr_{80}O_{320}$	S_3C_2	6.67	1255	5			$Sr_{85}Cr_{80}O_{312}$	S_3C_2	11.76
			SC	93.33						SC	85.92
										C	2.32
							1262	16	no change		
66.67	33.33	$SrCrO_4$	SC	100	1275	6			$SrCrO_{3.8}$	S_3C_2	9.10
										SC	86.36
										C	4.54
							1284	5	$SrCrO_{3.97}$	S_3C_2	1.36
										SC	97.96
										C	0.68
65	35	$Sr_{26}Cr_{28}O_{107}$	SC	96.29	1283	5			$Sr_{26}Cr_{28}O_{101.84}$	S_3C_2	8.57
			C	3.71						SC	82.97
										C	8.56
							1290	4	$Sr_{26}Cr_{28}O_{106.29}$	S_3C_2	1.05
										SC	94.66
										C	4.29
60	40	$Sr_6Cr_8O_{27}$	SC	85.71	1297	5			$Sr_6Cr_8O_{25.60}$	S_3C_2	8
			C	14.29						SC	72
										C	20
							1320	5	$Sr_6Cr_8O_{26.84}$	S_3C_2	1
										SC	84
										C	15

[a] Melted within 5 °C above liquidus temperature.
[b] Compositions melted in air and oxygen were reversed by reheating at 1125 °C in air.
[c] Calculated from the weight gains of melted specimens when reversed to their initial bulk composition (phase assemblage) at 1125 °C in air.
[d] Liquidus bulk compositions recalculated on the basis of mol percent $Sr_3Cr_2O_8$, $SrCrO_4$, and Cr_2O_3.
S_3C_2=$Sr_3Cr_2O_8$ SC=$SrCrO_4$ C=Cr_2O_3.

composition of the liquid lies at point *a* (fig. 4) which is within the $Sr_3Cr_2O_8$—$SrCrO_4$—Cr_2O_3 subternary and is represented by the "peritectic" between 68–67 mol percent SrO in figure 3. The "peritectic" is not binary but is merely the projection of point *a* which is the intersection of the 0.21 atm liquidus isobar and the boundary curve delimiting the primary fields of $SrCrO_4$ and Cr_2O_3 in the $Sr_3Cr_2O_8$—$SrCrO_4$—Cr_2O_3 subternary as shown in figure 4. Triangle $SrCrO_4$—*a*—Cr_2O_3 represents the univariant equilibria among $SrCrO_4$, liquid, $C_{E}2O_3$, and O_2 at 1251 °C and is represented by the 1251 °C "peritectic" horizontal in figure 3. As liquid *a* is not binary, specimens between $SrCrO_4$ and Cr_2O_3, quenched from solidus temperatures and above, show $Sr_3Cr_2O_8$ in their x-ray powder patterns. This manifestation of reduction was of particular importance in the determination of the 1251 °C solidus. The compound $PbCrO_4$, isostructural with $SrCrO_4$, decomposes in the solid state at low temperatures in air to Pb_2CrO_5 plus Cr_2O_3 with O_2 evolution without intervention of melting [16]. Hexavalent Cr in the presence of Sr is thus more stable, requiring temperatures to 1251 °C before reduction proceeds.

The 0.21 atm liquidus isobar is shown in figure 4. Commencing at the 1453 °C melting point of $Sr_3Cr_2O_8$, it follows the $Sr_3Cr_2O_8$—$SrCrO_4$ join through the eutectic (e_b). This portion of the system is strictly binary. Between the eutectic and 69 mol percent SrO, it migrates into the subternary across the primary field of $SrCrO_4$ to the $SrCrO_4$—Cr_2O_3 boundary curve (point a) from where it crosses the primary field of Cr_2O_3. Assuming that Cr_2O_3 melts congruently without oxygen loss in air at elevated temperatures, it terminates at the sesquioxide apex. It is, therefore, obvious that in figure 3, the liquidus curves (< 69 mol

% SrO) shown represent the described isobar in projection but only indicate the temperature at which a given phase assemblage melts. Compositions corresponding to each liquidus temperature can be deduced only with aid of the ternary.

Interpretation of figure 4 may be facilitated by two appropriate examples.

(a) Starting with a raw compositon of 68–32 mol percent SrO and Cr_2O_3, respectively, and heating in air at subsolidus temperatures results in the oxidation of available Cr^{3+} and the formation of a two phase mixture, $Sr_3Cr_2O_8 + SrCrO_4$, whose bulk composition lies on the $Sr_3Cr_2O_8$—$SrCrO_4$ tie line. At 1230 °C, initial melting occurs. Phases present are $Sr_3Cr_2O_8$, $SrCrO_4$, and binary eutectic liquid. As temperature is raised $Sr_3Cr_2O_8$ dissolves in the liquid and the phase assemblage consists of $SrCrO_4$ + binary liquid. Further elevation of temperature results in increased solubility of $SrCrO_4$ in the liquid which begins to evolve O_2 (reduce). As this occurs, the composition of the liquid follows the isobar into the ternary while bulk composition follows the 68 mol percent SrO oxygen reaction line. At about 1247 °C complete melting occurs in the primary field of $SrCrO_4$ and liquid composition and bulk composition (intersection of the isobar and the pertinent oxygen reaction line) coincide.

(b) Starting with a 2:1 mixture of SrO and Cr_2O_3 and heating in the subsolidus results in the complete oxidation of Cr^{3+} to Cr^{6+} and the formation of $SrCrO_4$. At 1251 °C, $SrCrO_4$ melts "incongruently" with O_2 evolution to Cr_2O_3 + liquid. Composition of the liquid is at point *a* in figure 4 while the bulk composition is located in the $SrCrO_4$—*a*—Cr_2O_3 triangle on the $SrCrO_4$ oxygen reaction line. The exact position has not been determined but at maximum heat content point *b* is representative. As temperature is raised, reduction in the liquid proceeds and its composition follows the air isobar as bulk composition continues along the oxygen reaction line. The equilibrium assemblage is Cr_2O_3 + liquid during this process. At about 1292 °C complete melting occurs and liquid and bulk composition coincide, again at the intersection of the air isobar and the pertinent oxygen reaction line.

4.2. 1 Atm O_2 Equilibria

Phase relations at 1 atm O_2 shown in figure 5, are not signifigantly different from those in air. Decrease of P_{H_2O}, inherent in the oxygen experiments, prevents the formation of apatite. Initially, it was anticipated that $Sr_3Cr_2O_8$ would show a low temperature minimum indicative of the possible oxidation reaction:

$$Sr_3Cr_2O_8 + \tfrac{1}{2}O_2 \rightarrow SrO + 2SrCrO_4$$

The compound, however, is stable to at least 715 °C in oxygen. The 775 °C minimum in air, therefore, is apparently due solely to the influence of water vapor. Melting relations in the SrO-rich portion of the system were not determined as they are expected to be identical to those in air. Confirmation of the 1230 °C solidus in air between $Sr_3Cr_2O_8$ and $SrCrO_4$ was made using the 68 mol percent SrO composition. The binary nature of the solidus is further validated, as this temperature does not increase in oxygen.

The 1 atm O_2 liquidus isobar (fig. 4) between $Sr_3Cr_2O_8$ and $SrCrO_4$ coincides with that join beyond 69 and 68 mol percent SrO. The join is, therefore, almost entirely binary in oxygen. $SrCrO_4$ melts sharply at 1283 °C but some reduction at the melting point was indicated by small amounts of $Sr_3Cr_2O_8$ found in diffraction patterns. Gravimetric experiments confirmed this observation. The compound melts in a "congruent" manner although melting is accompanied by O_2 evolution from the liquid. This indicates that the 1 atm O_2 isobar and the $SrCrO_4$ oxygen reaction line intersect in the primary field of $SrCrO_4$. Figure 6 schematically demonstrates the influence of oxygen pressure on the melting behavior of $SrCrO_4$.

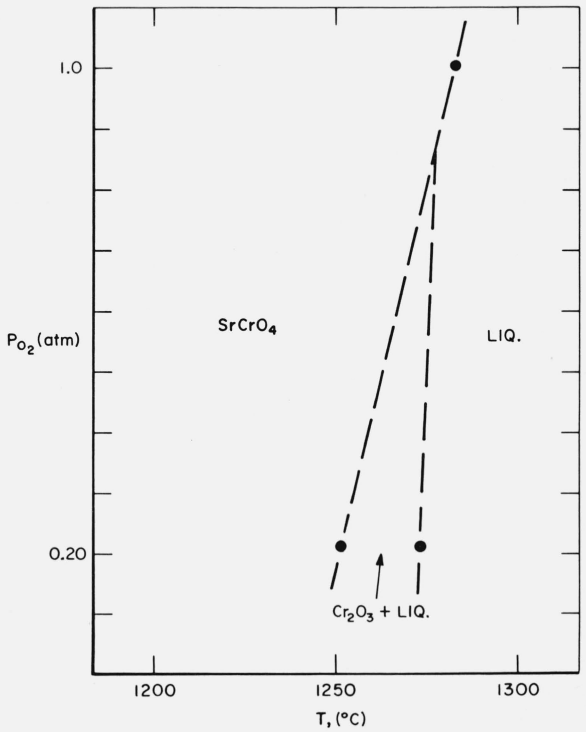

FIGURE 6. *Schematic representation of the melting behavior of* $SrCrO_4$ *between* 0.21 *and* 1 atm O_2.

Compositions of liquids are not indicated.

From a value of 1251 °C in air, the solidus temperature between $SrCrO_4$ and Cr_2O_3 is raised to 1275 °C and a "eutectic" appears to exist between 65 and 66 mol percent SrO. As $SrCrO_4$ and the 65 and 60 mol percent SrO compositions evolve O_2 at liquidus temperatures, the two segments of the 1 atm O_2 isobar may be extrapolated to an intersection on an oxygen reaction line pertinent to a composition initially between 65 to 66 mol percent SrO but within the ternary. This intersection delimits to within at least 1 mol percent the location (point *c*) of the $SrCrO_4$—Cr_2O_3 boundary curve at 1 atm O_2. In projection

(fig. 5) point c is the "eutectic" between 65 to 66 mol percent SrO. The 1 atm O_2 liquidus isobar coincides with the $Sr_3Cr_2O_8$—$SrCrO_4$ join to at least 68 mol percent SrO. Between this composition and $SrCrO_4$ it must migrate into the ternary (it cannot coincide with $SrCrO_4$ since the phase melts with O_2 loss), cross the primary field of $SrCrO_4$ to the boundary curve, and eventually terminate at Cr_2O_3.

The approximate position of the $SrCrO_4$—Cr_2O_3 boundary curve in figure 4 may be extrapolated toward the $Sr_3Cr_2O_8$ apex beyond point a. Similarly, the binary eutectic on the $Sr_3Cr_2O_8$—$SrCrO_4$ join must be a temperature maximum on that join (Alkemade theorum) and can, therefore, be extrapolated into the ternary. The resulting line, the $Sr_3Cr_2O_8$—$SrCrO_4$ boundary curve, where it intersects the $SrCrO_4$—Cr_2O_3 boundary curve, approximates the position of the $Sr_3Cr_2O_8$—$SrCrO_4$—Cr_2O_3 ternary eutectic. Another boundary curve, that between $Sr_3Cr_2O_8$ and Cr_2O_3, must, of course, converge at this point. A possible position is, therefore, indicated. It should be emphasized that the ternary invariant point is an integral portion of the system but is experimentally realized only at a fixed P_{O_2} and temperature. Similarly, for every P_{O_2}, a corresponding liquidus isobar exists within the ternary (as long as new phases do not appear). It is, therefore, obvious that every point on a boundary curve is characterized by a specific temperature and P_{O_2}. Having determined two such points (a, c) for the $SrCrO_4$—Cr_2O_3 boundary curve and the 1230 °C maximum on the $Sr_3Cr_2O_8$—$SrCrO_4$ boundary (e_b), values of < 0.1 atm O_2 and about 1210 to 1220 °C are not too improbable for the position of the ternary eutectic.

5. References

[1] Pistorius, C. W. F. T., and Pistorius, M. C., Zeit. Krist. **117,** 259 (1962).
[2] Scholder, V. B., and Schwarz, H., Z. anorg. allgem. Chem. **326,** 11 (1963).
[3] Wilhelmi, K. A., and Jonsson, O., Acta Chem. Scand. **19,** 177 (1965).
[4] Wilhelmi, K. A., Arkiv für Kemi **26,** 149 (1966).
[5] Wilhelmi, K. A., Arkiv für Kemi **26,** 157 (1966).
[6] Chamberland, B. L., Solid State Communications **5,** 663 (1967).
[7] Stimson, H. F., J. Res. NBS **65A** (Phys. and Chem.) No. 3, 139 (1961).
[8] Klemm, W., Angew. Chem. **63,** 396 (1951).
[9] Scholder, R., Angew. Chem. **65,** 240 (1953).
[10] Scholder, R., Angew. Chem. **70,** 583 (1958).
[11] Scholder, R. and Klemm, W., Angew. Chem. **66,** 461 (1954).
[12] Zachariasen, W. H., Acta Cryst. **1,** 263 (1946).
[13] Banks, E. and Jaunarajs, K. L., Inorg. Chem. **4, 78** (1965).
[14] Scholder, R. and Suchy, E., Z. anorg. allgem. Chem. **308,** 295 (1961).
[15] Randall, Jr., J. J. and Katz, L., Acta Cryst. **12,** 519 (1959).
[16] Negas, T., J. Am. Ceram. Soc., December (1968).

(Paper 73A4–562)